Society For Biomaterials

Channeled scaffolds implanted in adult rat brain

Cristina Martínez-Ramos,[1] Ana Vallés-Lluch,[1] José Manuel García Verdugo,[2,3] José Luis Gómez Ribelles,[1,4] Juan Antonio Barcia,[5]* Amparo Baiget Orts,[1] José Miguel Soria López,[3,6]* Manuel Monleón Pradas[1,4]*

[1]Centro de Biomateriales, Universidad Politécnica de Valencia, PO Box 22012, E-46071 Valencia, Spain
[2]Instituto Cavanilles, Universidad de Valencia, Polígono La Coma, E-46980 Valencia, Spain
[3]CIBER de Enfermedades Neurodegenerativas, Instituto Nacional de Salud Carlos III, Spain
[4]CIBER de Bioingeniería, Biomateriales y Nanomedicina, Instituto Nacional de Salud Carlos III, Spain
[5]Hospital Clínico San Carlos, C/ Profesor Martín Lagos, S/N. Madrid, Spain
[6]Facultad Ciencias de la Salud, Universidad CEU Cardenal Herrera, Avda Seminario 46113 Moncada, Valencia, Spain

Received 27 February 2012; revised 28 April 2012; accepted 3 May 2012
Published online 26 June 2012 in Wiley Online Library (wileyonlinelibrary.com). DOI: 10.1002/jbm.a.34273

Abstract: Scaffolds with aligned channels based on acrylate copolymers, which had previously demonstrated good compatibility with neural progenitor cells were studied as colonizable structures both *in vitro* with neural progenitor cells and *in vivo*, implanted without cells in two different locations, in the cortical plate of adult rat brains and close to the subventricular zone. *In vitro*, neuroprogenitors colonize the scaffold and differentiate into neurons and glia within its channels. When implanted *in vivo* immunohistochemical analysis by confocal microscopy for neural and endothelial cells markers demonstrated that the scaffolds maintained continuity with the surrounding neural tissue and were colonized by GFAP-positive cells and, in the case of scaffolds implanted in contact with the subventricular zone, by neurons. Local angiogenesis was evidenced in the interior of the scaffolds' pores. New axons and neural cells from the adult neural niche abundantly colonized the biomaterial's inner structure after 2 months, and minimal scar formation was manifest around the implant. These findings indicate the biocompatibility of the polymeric material with the brain tissue and open possibilities to further studies on the relevance of factors such as scaffold structure, scaffold seeding and scaffold placement for their possible use in regenerative strategies in the central nervous system. The development of neural interfaces with minimized glial scar and improved tissue compatibility of the implants may also benefit from these results. © 2012 Wiley Periodicals, Inc. J Biomed Mater Res Part A: 100A: 3276–3286, 2012.

Key Words: scaffold, biocompatibility, brain, angiogenesis, neural regeneration

How to cite this article: Martínez-Ramos C, Vallés-Lluch A, Verdugo JMG, Ribelles JLG, Barcia JA, Orts AB, López JMS, Pradas MM. 2012. Channeled scaffolds implanted in adult rat brain. J Biomed Mater Res Part A 2012:100A:3276–3286.

INTRODUCTION

Injury in the central nervous system (CNS) of mammals causes severe and irreparable disabilities due to failure of neural tissue regeneration. There is evidence that axons in the CNS do have some capacity to regrow after injury. The extent of this growth, however, is quite limited and variable, depending on the age of the subject and the severity of the lesion. Neural regeneration could commonly be seen after injury in young individuals.[1,2] By contrast, the adult CNS shows a very limited capacity for regeneration after injury.[3,4] Some studies have shown regeneration in the adult CNS following a microlesion, with regrowth of cut axons across the lesion site.[5–7] The reason why the adult CNS is nonpermissive for neural regrowth is thought to lie in a combination of factors: death of injured neurons, reduced capacity of adult neurons to grow when injured, presence of inhibitory factors,[8] and lack of the necessary trophic molecules for cell survival. Furthermore, a major problem in tissue regeneration is the revascularization of the site.[9,10]

It is now well known that neural progenitor cells reside in the adult brain[11–13] that they supply new neurons after injury processes,[14] and that cell turnover occurs within specific brain regions throughout adulthood.[15,16] This continuous neurogenic process is sustained by the life-long

*These authors contributed equally to this work.
Correspondence to: M. M. Pradas; e-mail: mmonleon@upvnet.upv.es
Contract grant sponsor: Spanish Fondo de Investigacion Sanitaria (Spanish Ministry of Health); contract grant numbers: CP04/00036 and PI05/075
Contract grant sponsor: Spanish Ministry of Science and Innovation; contract grant number: MAT2008-06434
Contract grant sponsors: Fundación Ramón Areces; Copernicus Program of University CEU-Cardenal Herrera; Regenerative Medicine Program Agreement between the Generalitat Valenciana and the Spanish National Health Institute Carlos III

persistence of neural stem cells (NSCs) within restricted CNS areas. In the adult mammalian brain the genesis of new neurons has been consistently documented in the subgranular layer of the dentate gyrus of the hippocampus, and in the subventricular zone (SVZ) of the lateral ventricles.[12,16–19] The telencephalic subventricular zone is the main neurogenic niche and the main source of adult neural stem cells.[20–24]

Still, the size of the lesion is a very important limiting factor in the process of regeneration. Large damages imply a loss of the tissue structures needed by the newly produced neural cells to migrate and rebuild the brain tissue.[25,26] To overcome this problem and favor the regeneration of neural tissue after CNS injury effort has been devoted to investigate the use of different types of polymeric scaffolds in the brain. Scaffolds made of hyaluronic acid, poly-(epsilon-caprolactone), poly(glycolic acid) or even polydimethylxilosane have been employed in animal models of cortical damage.[9,27–30] Recent studies stress that vascularization and local angiogenesis processes become crucial for a correct neuroregeneration strategy.[31] A suitable scaffold for tissue engineering in the brain should support cell growth, maintain differentiated cell functions, be highly porous and be as compliant as the host tissue; the porosity facilitates the accommodation of many cells,[29,32] enables a uniform distribution of the cells and the diffusion of oxygen and nutrients from host tissue, and must permit the neovascularization of the matrix if the cells inside it must survive.

As a tool in regenerative strategies, synthetic scaffolds may be useful as guides for axonal extension and as paths for migrating progenitor cells. They can also provide a shelter for neural cells against aggressive inflammatory local environments produced after trauma or degeneration processes. Promising results have been obtained with polymers used to repair neural defects in central and peripheral nervous tissues.[33–35] The degree of hydrophilicity of the artificial substrate has a strong influence on cell behavior. We have previously investigated the ability of synthetic substrates based on copolymers of poly(ethyl acrylate) (PEA) and poly (hydroxyl ethyl acrylate) (PHEA) to sustain survival and neuronal differentiation of NSCs and other neural cells,[36–38] with the aim of selecting a chemical composition suitable for the fabrication of more complex scaffolding structures. That work studied the influence of the hydrophilicity on cell behavior in the acrylate copolymer family and led us to conclude that the more hydrophobic compositions behaved as better substrates for cell adhesion, whereas the more hydrophilic ones were much less suited for cell adhesion. On the basis of those findings, we designed three-dimensional channeled scaffolds based on a PEA-PHEA copolymer, and in the present work we investigated whether neural cells could colonize these polymeric scaffolds both *in vitro* and *in vivo*, when the scaffolds were implanted in two regions of different neurogenic potential: the cerebral cortex and in the proximity of the SVZ neural niche. We characterized the cell typologies invading the scaffold when seeded *in vitro* with neural precursors (neurospheres); we have ascertained *in vivo* the ability of the colonizing cells to promote neurite extension and local angiogenesis within the synthetic structures.

MATERIALS AND METHODS

Preparation and characterization of the channeled scaffolds

Two different types of channeled scaffolds were prepared following a porogen-template leaching method as described in Refs. 39–41. The first scaffold structure consisted in a matrix with unidirectionally aligned parallel cylindrical isolated channels [type I scaffolds, Fig. 1(A,B)]; the second structure consisted in a matrix with interconnected orthogonal cylindrical pores in the three spatial directions [type II scaffolds, Fig. 1(C,D)].

The polymer matrix for both types of structure was the same: a copolymer of ethyl acrylate (EA) and hydroxyethyl acrylate (HEA) with EA:HEA mass ratio of 9:1, crosslinked to form a network with ethyleneglycol dimethacrylate (EGDMA) in a mass ratio of (EA+HEA):EGDMA = 99:1. The matrix precursor reactants mixture consisted in monomers of EA, (99% pure, Sigma–Aldrich, Spain), HEA, (99% pure, Sigma–Aldrich, Spain) and EGDMA (98% pure, Sigma–Aldrich, Spain), all of them used as received without further purification, in the mass ratios specified above. To this mixture azo-bis-isobutyronitrile, AIBN, (Merck, 98% pure) in weight percentage of 0.01% was added to act as thermal initiator of the polymerization. Moulds with the different porogen templates were filled with this reactant mixture, and the polymerization was carried out for 24 h at 60°C, and for 24 h more at 90°C.

The moulds for type I scaffolds were prepared as follows: glass tubes of 4 mm inner diameter were cut in 3.5-cm long pieces, stuffed with 40 μm diameter polyacrylonitrile (PAN, Montefibre Hispania SA, Spain) aligned fibers in the direction of the tube axis, and sealed on one side. The reactant mixture described above was vacuum-injected into these glass moulds, which were immediately capped and placed in an oven for polymerization. After completion of the polymerization the PAN fibers were eliminated from the materials by dissolution in *N*,*N*-dimethylformamide (99.8%, Aldrich, Spain). The resulting scaffolds were washed in boiling ethanol for 24 h to remove residuals and nonreacted monomers, and were finally dried in a vacuum desiccator at 80°C until constant weight. For use in the experiments, both *in vitro* and *in vivo*, 1-mm thick cylinders cut normal to channel direction were cut from the obtained samples; from these sections, pieces of 4 mm × 1 mm were cut. Thus, the scaffold pieces for the experiments were in the form of bars with approximate dimensions of 1 mm thickness and faces of 4 mm × 1 mm normal to pore direction.

The moulds for type II scaffolds were prepared as follows: a porogen template was produced by sintering piled sheets of Nylon fabrics (Saati SA, Barcelona, Spain) with nominal thread diameter of 80 μm and mesh opening of 120 μm; this template was placed between glass plates to obtain a 3D mould. The previously prepared reactant

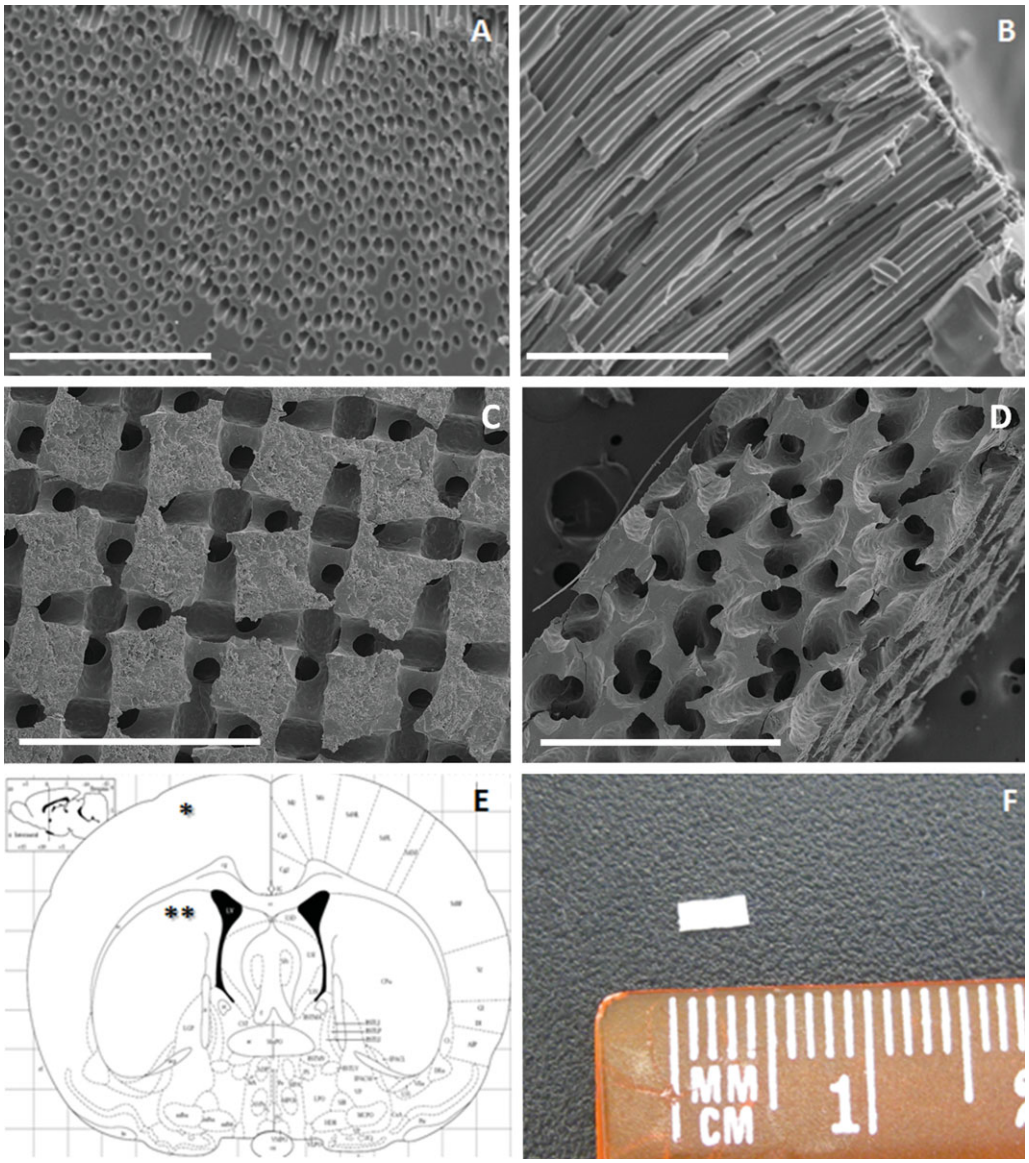

FIGURE 1. A,B: Electron micrographs of type I scaffold, a matrix with parallel isolated cylindrical pores. C,D: Electron micrographs of type II scaffold, a matrix with interconnected cylindrical pores laid out in an orthotropic three-dimensional arrangement. E: scheme showing the different positions of the implants in the brain, placement in cerebral cortex (*) and near the SVZ (**). F: bright field microphotograph of implant piece of type II scaffold. Scale bar = 300 μm in A, B and 800 μm in C, D. [Color figure can be viewed in the online issue, which is available at wileyonlinelibrary.com.]

mixture was injected into these moulds and polymerized at the above mentioned conditions. After polymerization the obtained sheets were cut into smaller pieces and rinsed in nitric acid (65%, Scharlab, Spain) under gentle shaking for 48 h to dissolve the fiber template. Finally, the obtained materials were washed in boiling ethanol for 40 h, and dried 24 h at room temperature, a further 24 h under vacuum and room temperature, and 24 h more under vacuum at 60°C. From the ~1-mm-thick sheets thus obtained pieces in the form of bars with faces of 4 mm × 1 mm were cut and used in all the experiments [Fig. 1(F)].

All scaffold samples were sterilized with a 25 kGy dose of gamma irradiation in a ^{60}Co source (Aragogamma, Barcelona, Spain).

In vitro culture of neural stem cells in scaffolds

Neural stem cell cultures were established as previously described.[36] Tissues obtained from the SVZ of postnatal rats were mechanically dissociated with a fire-polished Pasteur pipette. Cell suspensions at a surface density of 8000 cells cm^{-2} were cultured in DMEM/F12 basal medium in the presence of epidermal growth factor (EGF) and fibroblast growth factor (FGF). The spheres formed (neurospheres) were collected and dissociated every 2–3 days and the total number of viable cells was assessed at each passage by trypan blue (Sigma) exclusion. Cells at passage 3 were mechanically dissociated into single cells and cultured without EGF and FGF at 12,000 cells cm^{-2} according to the Gritti and Vescovi method,[42] and seeded into the different

biomaterials. First 30 μL of concentrated neural cells suspension were laid on the scaffold, and incubated for 1 h at 37°C and 5% CO_2 to enhance seeding efficiency; after this time, 300 μL of medium were added to each well and changed every 2 days. The culture was evaluated at day 5.

In vivo scaffold implantation

Eight-week-old Wistar female rats, weighing ~220–250 g, were used for the experiments. Animals were anesthetized with 3.0% and maintained in 0.4–0.8% isoflurane in 70% N_2O and 30% O_2 and immobilized in a stereotactic head frame with the incisor bar set. All surgical and experimental procedures were approved by the institution's Ethical Committee. Under aseptic conditions, a midline incision was made taking the bregma as reference point.[43] A 4-mm diameter bone trap was performed to 1 mm from bregma and 1 mm right of midline. A block of cortical tissue (1.0 mm × 4.0 mm × 1.0 mm) was removed mechanically with an excavator spoon and a lesion was made in the frontal region of the brain. An empty, unseeded acrylic scaffold of dimensions 1.0 mm × 4.0 mm × 1.0 mm [Fig. 1(F)] was placed into the lesion site.

Animals were divided in two groups ($n = 8$ each) according to the lesion site. In a first group, the lesion was performed in the outer part of the cerebral cortex at 3 mm ventral to the skull at the midline. A second group was injured more deeply (at 6 mm ventral), close to the SVZ, see Figure 1(E). For both groups control animals were intervened and left without implant.

Tissue preparation and histology

After 8 weeks, animals were perfused transcardially with 4% paraformaldehyde (PFA) and the excised brains were postfixed with 4% PFA at 4°C overnight. Then, brains were cryoprotected by immersion in PBS 0.1 *M* and pH 7.5 containing 30% sucrose for 3 days and included in OCT. 20 μm coronal sections were obtained by using a cryostat (Leica, CM 1900) and collected onto superfrost slides. After washing with PBS 0.1*M* (3 × 5 min) sections were processed for hematoxilin–eosine staining to reveal the presence of neural cells within scaffolds.

Immunohistochemistry

The *in vitro* cultures on acrylic scaffolds and the sections from the *in vivo* assays were processed for inmunohistochemistry. Samples were washed with 0.1*M* sodium phosphate buffer (PBS, pH 7.4) and postfixed for 10 min in 4% paraformaldehyde. After 30 min permeabilization (10% fetal bovine serum and 0.1% triton X-100 in PBS) samples were incubated with the different primary antibodies. Anti-neural class IIIB-tubuline (Babco, cat n° MM-S405-P, 1:500), anti-NeuN (Chemicon, cat n° MAB377,1:100), anti-glial fibrillary acidic protein (GFAP Sigma, cat n° G-3893, 1:500), and anti-CD31 (BD Bioscience Farmingen, cat n° 550300, 1:50) were incubated overnight at 4°C in a humidified chamber. After rinsing in 0.1*M* PBS, cells were incubated for the secondary antibodies goat anti-rabbit cyanine conjugated Cy2 or goat anti-mouse cyanine conjugated Cy3 (Jackson Immunoresearch, 1:200) during 1 h. Nuclei were counterstained with DAPI (4′,6-diamidino-2-phenylindole, Sigma, 1:5000). After additional washes, the stained samples were observed in a microscope equipped for epifluorescence (Leica DM600). Images were obtained with a digital camera (Leica 480×). To better study the cell morphology of NSCs images were obtained by confocal microscopy (Leica TCS SP2 AOBS inverted confocal microscope).

RESULTS

Adult neural stem cells colonize the scaffold and differentiate into neurons and glial cells within the channels *in vitro*

The adult neural stem cells were able to completely colonize the scaffolds' channels during the culture time analyzed, and exhibited good adhesion and survival. These neurospheres are known to give rise to differentiated neurons, astrocytes, and oligodendrocytes. After 5 days *in vitro* culture within the parallel-channel (type I) scaffolds the NSCs obtained from the neurospheres differentiated into young neurons immunoreactive for the neuronal markers NeuN [Fig. 2(A)] and Tuj-1 [Fig. 2(B,D)] and astrocytes [Fig. 2(D)], which appeared distributed over the scaffold's exterior surfaces and within the channels. Completely similar results were obtained with the type II scaffolds.

Integration of the scaffolds in the cortical region

Under the specific stereotactic coordinates specified above scaffolds were implanted in two different locations to study the distinct neurogenic potential of both regions. Figure 1(E) shows a scheme of the scaffold position (asterisks) after its placement near the SVZ (**) and in the cortex (*) of the adult rat brains.

GFAP reactivity reflects the astrocyte population around and within the biomaterial. After 8-week implantation, the density of GFAP-positive cells enveloping the biomaterial was not abnormally high, both for the materials implanted in the cortical region [Fig. 3(C)] and near the SVZ [Fig. 3(D)]; thus, the brain tissue response and the inflammatory reaction subsequent to the surgical implantation were moderate, did not lead to an impervious glial scar, and permitted an excellent integration of the material [Fig. 3(A,B)]: the typical slight inflammatory reaction following any surgical injury in the CNS was observed in the first days (data no shown), but it had almost disappeared after 8 weeks, leaving the artificial matrices surrounded by a thin layer of astrocytic cells. The results show cells infiltrating the channels and around the implant; but in comparison with the materials implanted near the SVZ [Fig. 3(D)] in the cortex the degree of colonization was significantly less, with empty noncolonized spaces visible inside the scaffold [white arrows in Fig. 3(C)]. In all cases, however, the implants remained firmly adhered to the host brain.

Integration of the scaffolds implanted near the SVZ

In the case of the materials implanted near the SVZ, after 2 months it was possible to observe cells abundantly

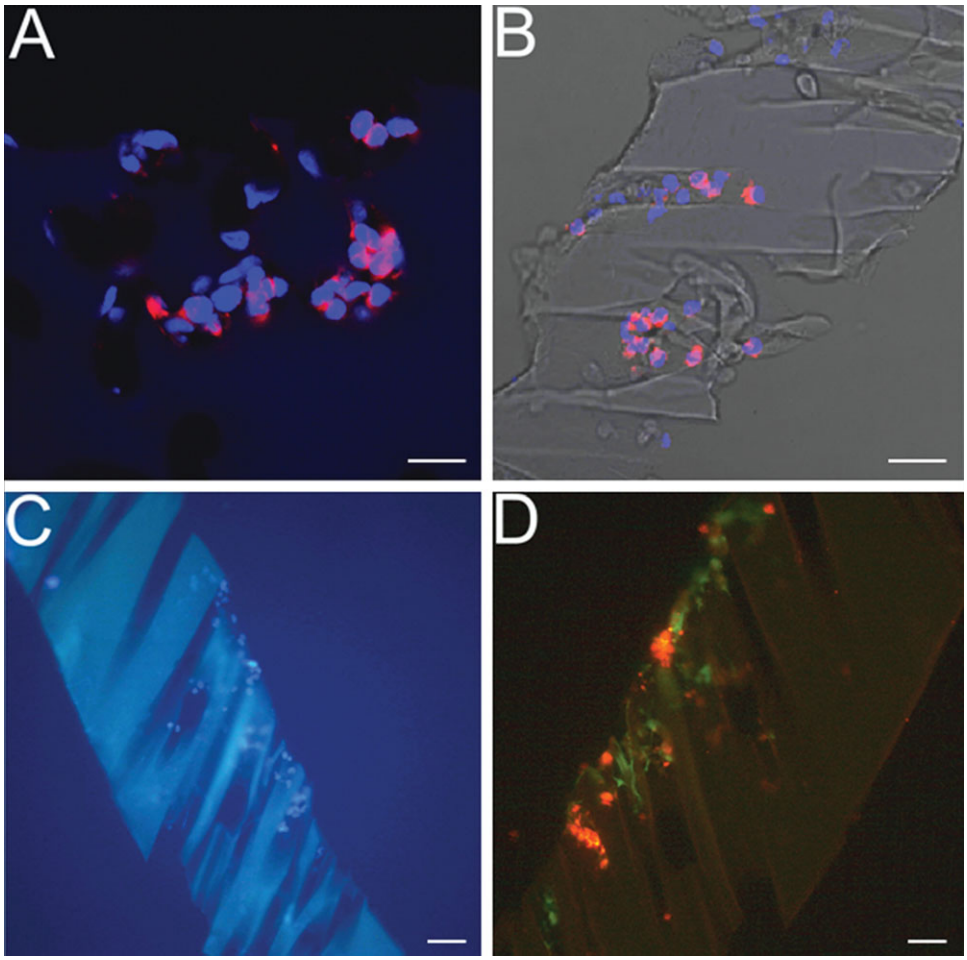

FIGURE 2. Fluorescence microscope image of channeled type I scaffold seeded with neural stem cells after 5 days. Glial cells and neurons were found colonizing the lumina of the pores: differentiated neurons immunoreactive for NeuN (red in A) and Tuj-1 (red in B, D), and GFAP+ glial cells (green in D). Nuclei stained in blue with DAPI. Scale bar = 100 μm in A, D and 200 μm in B, C. [Color figure can be viewed in the online issue, which is available at wileyonlinelibrary.com.]

colonizing the scaffolds in the interior of the channels [Figs. 3(D) and 4(A,B), cells stained with hematoxylin]. GFAP-positive astrocytes were observed surrounding the implant, but they did not constitute a developed scar [Fig. 4(C)], and they did not impede the colonization of the channels by others cells [Fig. 4(D–F)]. Confocal microscopy revealed elongated neurites immunoreactive for Tuj-1 [in red, white arrows in Fig. 4(F)] that colonized the interior of the scaffold channels. Besides, these young neurons (inmunopositive for Tuj-1marker) that had migrated into the scaffold were observed to be in contact with GFAP inmunoreactive astrocytes [in green, head arrows in Fig. 4(F)]. Even though in all cases the biomaterials were well attached to the surrounding tissue, as evaluated from the brain sections stained and treated for immunohistochemistry, the results of this group (implants near the SVZ) showed a better colonization and cell infiltration by neural cells than the other group (implants in the cortex). Thus, degree of integration and cell invasion of the implants were significantly different at both implant sites.

Neural cells and neoangiogenesis within scaffolds implanted near the SVZ

To further characterize the kind of the cells colonizing the scaffold after 2 months, brain coronal sections were analyzed for neuronal (Tuj-1) and endothelial cell markers (CD31). The sections containing the biomaterials implanted close to the SVZ permitted the transversal observation of the channels [Fig. 5(D)]. After 2 months new neurons and blood vessels could be found within the channels (Figs. 5 and 6). In a bright field microphotograph [Fig. 5(A)] the biomaterial placed close to the SVZ can be seen to be continuously integrated with the surrounding neural tissue and to be completely colonized by numerous cells stained with DAPI [nuclei in blue in Fig. 5(B)]. A detailed image [Fig. 5(C,D)] evidences the presence of new vessels formed by CD31-positive cells [white arrows in Fig. 5(C,D)]. Vessels were observed to be distributed randomly along the scaffold channels [Fig. 5(D)]. Tuj-1+ neurons with elongated form (migratory-like neurons) were found inside the channels with an intimate contact of the astrocytes (Fig. 6). Moreover,

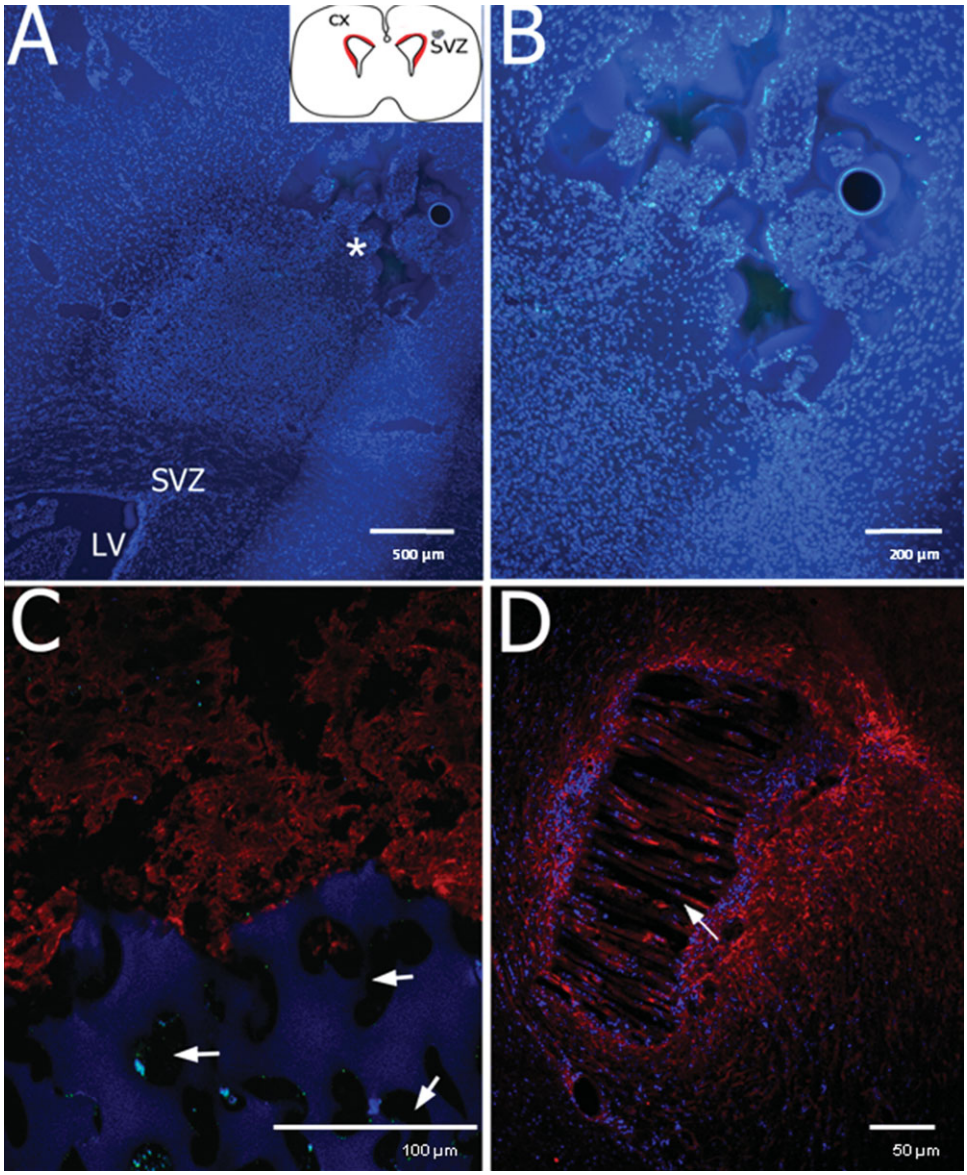

FIGURE 3. Integration of the scaffolds in the host tissue after 8-week implantation. A–C: type II scaffolds implanted in the brain cortex region: DAPI staining (blue in A and B, which is a magnification of A) reveals an intimate contact between the scaffold (asterisk in A) and the surrounding tissue. A thin glial scar (GFAP-positive cells in red) could be seen around the scaffold (C, D). Pores of the scaffolds implanted in the cortical zone appeared sometimes devoid of cells (arrows in C) when compared with the scaffolds implanted near the SVZ (D shows a type I scaffold implant). Scale bar = 500 μm in A, D; 100 μm in B and 50 μm C. [Color figure can be viewed in the online issue, which is available at wileyonlinelibrary.com.]

numerous axons [white arrows in Fig. 6(D)] and young neurons [white arrowheads in Fig. 6(A,B,D)] were observed at the scaffold-tissue interface close to the SVZ and entering from the host tissue into the scaffold, demonstrating the permeability of this structure.

DISCUSSION

Tissue engineering in the brain has become possible since the discovery of the—though limited—actual regeneration potential of neural stem cells residing in the adult organ.[44] This has raised founded expectations for cell therapy strategies in many CNS diseases.[45–48] However, pure cell supply strategies do not seem for the moment to achieve the desired results, and they are proving to be insufficient for axonal growth and neural reconnection across long distances.[49] Here is where synthetic biomaterials may be of help, in that they may provide both a sheltering environment that protects the regenerating tissue against the inflammatory and aggressive medium in the lesion and a guiding structure for the oriented growth of neuronal networks. This is why it is important to test the compatibility of CNS-neural cells and synthetic structures possessing both a cell-friendly chemistry and well-defined pore architecture. The response of neural cells to the chemistry of the scaffold materials of the present study was investigated in previous studies[36–38]; footing on those results we undertook to manufacture

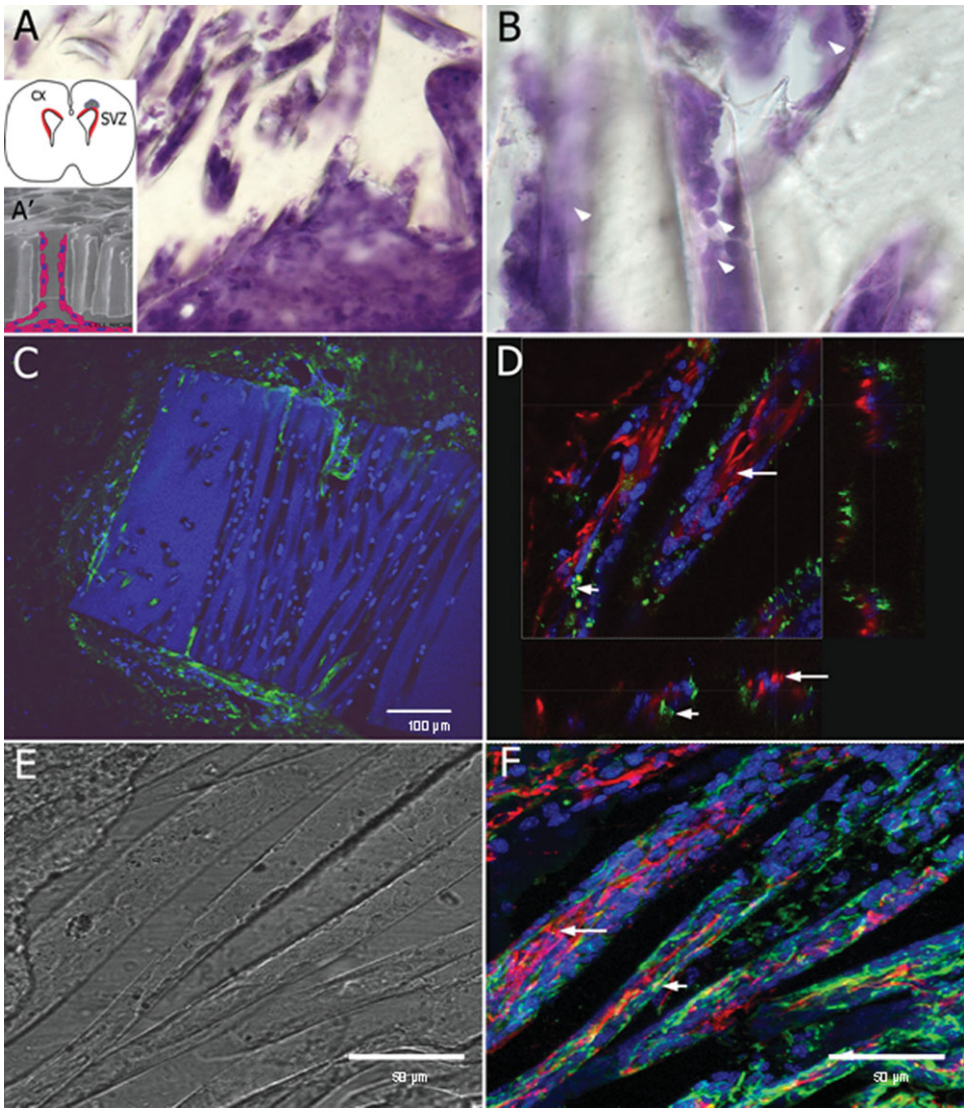

FIGURE 4. Type I scaffolds implanted 8 weeks near the SVZ. A and B: Optical micrograph of a section stained with hematoxilin to reveal the presence of neural cells (the gray spot in the scheme of A indicates scaffold location; the SVZ is singled out in red in the scheme). Cells are shown at the scaffold–tissue interface (A), and a detail of a channel (B) reveals numerous cells (scheme A′ in the insert to Figure A). C: Glial cells immunoreactive for GFAP (green) in around the scaffold. D–F: Reconstruction by confocal images of the longitudinal channels showing Tuj-1+ neurons (white arrow in D, F). GFAP+ glial cells (arrowhead in F) and CD 31+ cells could be seen inside the channels, suggesting the presence of some new blood vessels (arrowhead in D). Blue in C, D, F: nuclei stained with DAPI. Scale bar = 100 μm in C, and 50 μm in E, F.

scaffolds possessing two definite different porous structures bearing some resemblance to two important types of circuitry structures in the brain: that of the cortex, where neuronal interconnections follow a pattern of rows and columns more or less orthotropic, and that of axonal fascicles and tracts (such as the nigro-striatal pathway), where axons run in parallel bundles.[50] These two morphologies correspond to the two types of scaffolds here prepared [see Fig. 1(A–D)]. Type II scaffolds reproduce an approximately orthotropic pattern of cylindrical interconnected pores, whereas the pores of type I scaffolds are straight, parallelly aligned isolated cylinders. Whereas the parallelly aligned channels of type I scaffold represent a porous structure suited to guide axonal outgrowth and reconnect neuronal centers across some distance, the porous structure of type II scaffold is able to lodge a larger number of cells in an interconnected multilayered 3D arrangement, and could thus be more appropriate to provide cell lodging in the case of more extensive tissue damage. Both types of porous structures differed by the diameter of their typical pores and also by their interconnectivity. The results of cell cultures and of the *in vivo* implants demonstrate that these differences have no consequence on their invasibility by the cells, since both structures were abundantly colonized. In this respect, the most restrictive case *a priori* was represented by the type I scaffolds, because of their smaller pore diameter (40 μm vs. 80 μm in type II scaffolds) and of the lack of pore-to-pore interconnection. The scaffolds

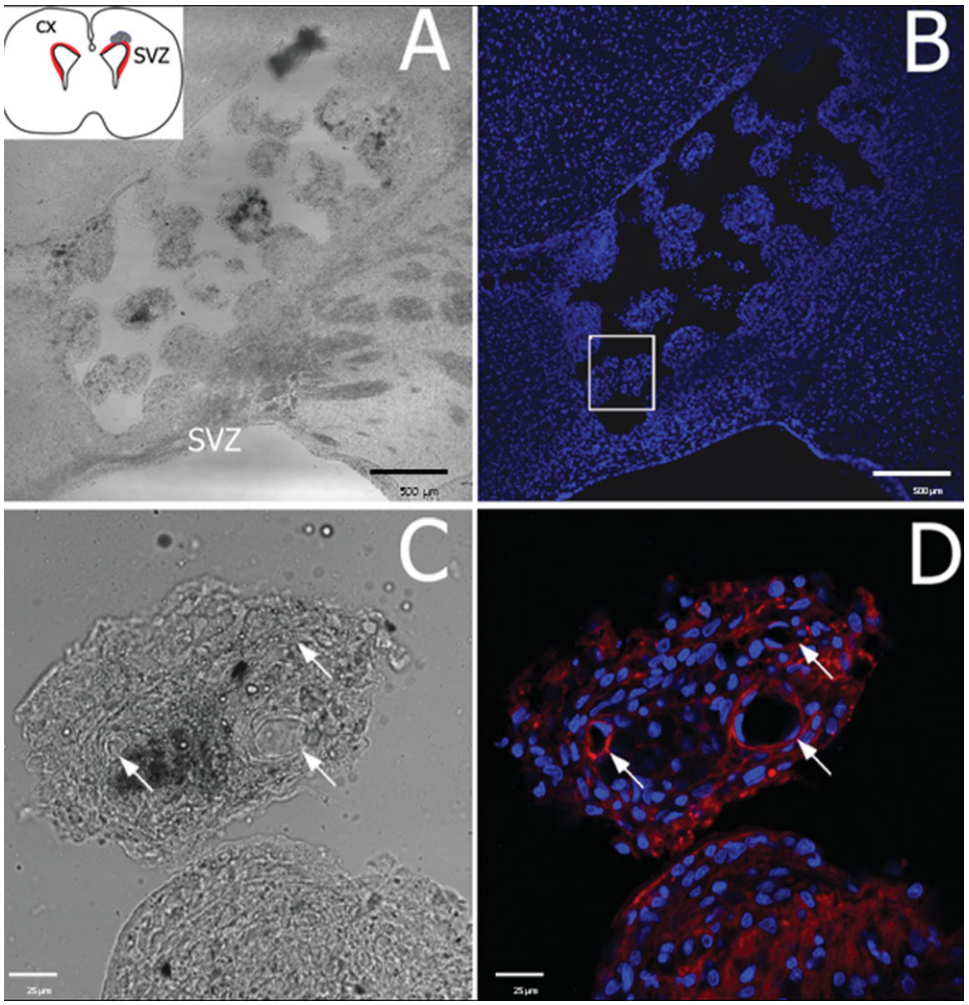

FIGURE 5. Type II scaffolds implanted close to the SVZ after 8 weeks. Bright field micrograph of a brain section (A,C). Scaffold pores were abundantly and uniformly colonized by cells (**A**, blue DAPI staining in B). Fluorescence image (D) showing a detail of a channel with vessel-like structures formed by endothelial cells (white arrows in C, D) immunoreactive for endothelial marker CD31 (red in D). Blue in B, D: nuclei stained with DAPI. Scale bar = 500 μm in A, B and 25 μm in C, D. [Color figure can be viewed in the online issue, which is available at wileyonlinelibrary.com.]

sustained, this notwithstanding, differentiated neural cells both *in vitro* and *in vivo*, in this last case during 8 weeks, which implies an efficient nutrient and metabolyte transport through and along the pores, guaranteed by sufficient microvessel formation: angiogenesis took place within the cylindrical pores, as ascertained directly by the specific endothelial cell markers [Figs. 4(D,F) and 5(D)] and indirectly by the very survival of the cells. This is a remarkable finding, since it was by no means at the outset clear that capillaries could form within these types of synthetic structures, characterized by long individual cylindrical pores only weakly interconnected (type II scaffolds, where parallel channels are communicated by perpendicular throats at spacings of 120 μm) or not interconnected at all (type I scaffolds). This process of angiogenesis may have been stimulated by a local hypoxic environment within the channels, since these represent long completely impervious cylindrical surfaces (type I scaffolds) or only interconnected at the intersection points of the channels (type II scaffolds); hypoxic conditions are known to stimulate the migration ad differentiation of endothelial cells and their progenitors.[51,52] On the whole, the neovessels inside the scaffold's pores and the long term survival of differentiated neurons and glial cells imply a pervious implant–host tissue interface, with no significant glial scar, through which numerous passing axons could be identified (Fig. 6).

The *in vitro* and *in vivo* colonizability of these structures is of relevance for the philosophy of cell therapy in the brain. *In vitro* the structures were able to host viably neural cells uniformly populating the material, which could thus become a vector for cell transplantation. *In vivo*, though the scaffolds had been implanted devoid of cells, they were abundantly colonized by neural cells *in vivo*, mostly GFAP-positive astrocytes. These cells could have originated from neural stem cells which migrate from proliferative sites to sites of lesion,[13,53] or they could be the descendants of cells drained into the pores of the material during the surgical process of implantation. Our experiments are insufficient to

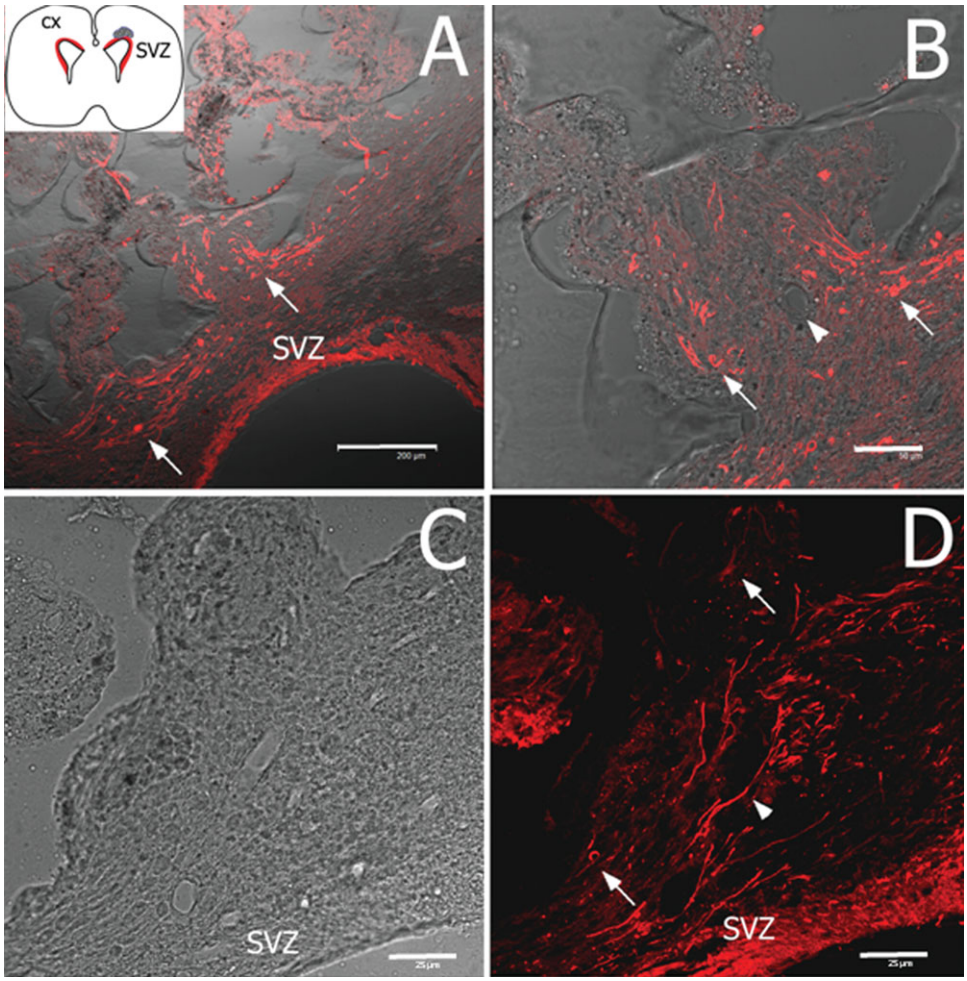

FIGURE 6. Scaffold–tissue interface of type II scaffolds implanted close to the SVZ after 8 weeks. Merged confocal images (red in A, B) of neural cells within the scaffold's pores, showing Tuj-1+ neurons (white arrows in A, B, D) crossing the glial interface and entering the implant. Scale bar = 200 μm in A; 50 μm in B and 25 μm in C,D. [Color figure can be viewed in the online issue, which is available at wileyonlinelibrary.com.]

decide on this matter. The latter hypothesis seems more plausible as an explanation for the origin of the endothelial cells and neovessels inside the pores, as surgery always entails the rupture of the blood-brain-barrier and the consequent bleeding and angiogenesis at the lesion margins; however, the migratory hypothesis has more weight for the origin of the other neural cells inside the channels, in the light of the different colonization patterns that the scaffolds exhibited when implanted near the SVZ (a highly proliferative region) and close to the cortex: these last were significantly less colonized than the former ones [Fig. 3(C,D)]. In any case, those cells were viable within the synthetic millimeter-sized structures, which testimonies to a rapid and efficient spontaneous vascularization of the implants that enabled cell nutrition and metabolism. The guess suggests itself that material structures encountered by cells in their migratory routes may conform the final geometrical pattern of their networks. Whether an exterior cell supply is necessary or not for the reconstruction of certain tissue structures, and whether this necessity depends on their anatomical location is a question of greatest importance for the philosophy of cell therapy; though not conclusive in any sense, our results help pose the problem in a way that further experiments may explore.

CONCLUSIONS

The acrylate chemistry is highly compatible with neural stem cells (as it is also with other cells[36–38]), both *in vitro* and *in vivo*. Channeled scaffolds made out of them with pore diameters in the range from 40 to 80 μm and pore geometries resembling typical brain structures achieve a uniform colonization by neural cells. Neural stem cells seeded *in vitro* within them differentiate to viable neurons and glial cells. When implanted *in vivo*, the scaffolds integrate into the host tissue without any dense glial scar or any type of appreciable discontinuity; the scaffold–tissue interface is pervious to neurons and axons, and the geometrical layout of the pore structure organizes the growth of the tissue. The colonization density pattern seems to be higher when the implant is close to the SVZ, suggesting that the cells colonizing the scaffold's pores originated in the nearby proliferative regions. The observed long term

viability of the neural cells within the pores is maintained by neovessels formed within the scaffold, probably from brain microvascular endothelial cells proceeding from the breakdown of the blood–brain-barrier during the injury. The scaffolds' pore geometries and sizes permitted this neovascularization within both types of constructs.

ACKNOWLEDGMENTS

The authors acknowledge an anonymous referee for pointing out the possible role of the pore geometry in creating a hypoxic environment that favors neoangiogenesis. They thank Alberto Hernandez Cano and Eva M[a] Lafuente Villarreal at CIPF for technical assistance and their knowledge of confocal microscopy.

REFERENCES

1. Cadelli DS, Bandtlow CE, Schwab ME. Oligodendrocyte- and myelin-associated inhibitors of neurite outgrowth: Their involvement in the lack of CNS regeneration. Exp Neurol 1992;115:189.
2. Nishio T. Axonal regeneration and neural network reconstruction in mammalian CNS. J Neurol 2009;256:306.
3. Davies SJ, Silver J. Adult axon regeneration in adult CNS white matter. Trends Neurosci 1998;21:515.
4. Huebner EA, Strittmatter SM. Axon regeneration in the peripheral and central nervous systems. Results Probl Cell Differ 2009;48:339.
5. Huang DW, McKerracher L, Braun PE, David S. A therapeutic vaccine approach to stimulate axon regeneration in the adult mammalian spinal cord. Neuron 1999;24:639.
6. McKerracher L. Spinal cord repair: Strategies to promote axon regeneration. Neurobiol Dis 2001;8:11.
7. Olakowska E, Woszczycka-Korczynska I, Jedrzejowska-Szypulka H, Lewin-Kowalik J. Application of nanotubes and nanofibres in nerve repair. A review. Folia Neuropathol 2010;48:231.
8. Bandtlow CE. Regeneration in the central nervous system. Exp Gerontol 2003;38:79.
9. Zhang H, Hayashi T, Tsuru K, Deguchi K, Nagahara M, Hayakawa S, Nagai M, Kamiya T, Osaka A, Abe K. Vascular endothelial growth factor promotes brain tissue regeneration with a novel biomaterial polydimethylsiloxane-tetraethoxysilane. Brain Res 2007;1132:29.
10. Kemp SW, Syed S, Walsh W, Zochodne DW, Midha R. Collagen nerve conduits promote enhanced axonal regeneration, Schwann cell association, and neovascularization compared to silicone conduits. Tissue Eng Part A 2009;15:1975.
11. Alvarez-Buylla A, Garcia-Verdugo JM. Neurogenesis in adult subventricular zone. J Neurosci 2002;22:629.
12. Alvarez-Buylla A, Garcia-Verdugo JM, Tramontin AD. A unified hypothesis on the lineage of neural stem cells. Nat Rev Neurosci 2001;2:287.
13. Garcia-Verdugo JM, Llahi S, Ferrer I, Lopez-Garcia C. Postnatal neurogenesis in the olfactory bulbs of a lizard. A tritiated thymidine autoradiographic study. Neurosci Lett 1989;98:247.
14. Marti-Fabregas J, Romaguera-Ros M, Gomez-Pinedo U, Martinez-Ramirez S, Jimenez-Xarrie E, Marin R, Marti-Vilalta JL, Garcia-Verdugo JM. Proliferation in the human ipsilateral subventricular zone after ischemic stroke. Neurology 2010;74:357.
15. Alvarez-Buylla A, Lim DA. For the long run: Maintaining germinal niches in the adult brain. Neuron 2004;41:683.
16. Doetsch F, Scharff C. Challenges for brain repair: Insights from adult neurogenesis in birds and mammals. Brain Behav Evol 2001;58:306.
17. Doetsch F. The glial identity of neural stem cells. Nat Neurosci 2003;6:1127.
18. Doetsch F, Caille I, Lim DA, Garcia-Verdugo JM, Alvarez-Buylla A. Subventricular zone astrocytes are neural stem cells in the adult mammalian brain. Cell 1999;97:703.
19. Kornack DR, Rakic P. The generation, migration, and differentiation of olfactory neurons in the adult primate brain. Proc Natl Acad Sci USA 2001;98:4752.
20. De Marchis S, Temoney S, Erdelyi F, Bovetti S, Bovolin P, Szabo G, Puche AC. GABAergic phenotypic differentiation of a subpopulation of subventricular derived migrating progenitors. Eur J Neurosci 2004;20:1307.
21. Garcia-Verdugo JM, Doetsch F, Wichterle H, Lim DA, Alvarez-Buylla A. Architecture and cell types of the adult subventricular zone: In search of the stem cells. J Neurobiol 1998;36:234.
22. Johansson CB, Momma S, Clarke DL, Risling M, Lendahl U, Frisen J. Identification of a neural stem cell in the adult mammalian central nervous system. Cell 1999;96:25.
23. Reynolds BA, Weiss S. Generation of neurons and astrocytes from isolated cells of the adult mammalian central nervous system. Science 1992;255:1707.
24. Xu Q, de la Cruz E, Anderson SA. Cortical interneuron fate determination: Diverse sources for distinct subtypes? Cereb Cortex 2003;13:670.
25. Lakatos A, Barnett SC, Franklin RJ. Olfactory ensheathing cells induce less host astrocyte response and chondroitin sulphate proteoglycan expression than Schwann cells following transplantation into adult CNS white matter. Exp Neurol 2003;184:237.
26. Papadopoulos CM, Tsai SY, Alsbiei T, O'Brien TE, Schwab ME, Kartje GL. Functional recovery and neuroanatomical plasticity following middle cerebral artery occlusion and IN-1 antibody treatment in the adult rat. Ann Neurol 2002;51:433.
27. Hou S, Xu Q, Tian W, Cui F, Cai Q, Ma J, Lee IS. The repair of brain lesion by implantation of hyaluronic acid hydrogels modified with laminin. J Neurosci Methods 2005;148:60.
28. Park KI, Teng YD, Snyder EY. The injured brain interacts reciprocally with neural stem cells supported by scaffolds to reconstitute lost tissue. Nat Biotechnol 2002;20:1111.
29. Tian WM, Hou SP, Ma J, Zhang CL, Xu QY, Lee IS, Li HD, Spector M, Cui FZ. Hyaluronic acid-poly-D-lysine-based three-dimensional hydrogel for traumatic brain injury. Tissue Eng 2005;11:513.
30. Wong DY, Krebsbach PH, Hollister SJ. Brain cortex regeneration affected by scaffold architectures. J Neurosurg 2008;109:715.
31. Morgan R, Kreipke CW, Roberts G, Bagchi M, Rafols JA. Neovascularization following traumatic brain injury: Possible evidence for both angiogenesis and vasculogenesis. Neurol Res 2007;29:375.
32. Woerly S, Petrov P, Sykova E, Roitbak T, Simonova Z, Harvey AR. Neural tissue formation within porous hydrogels implanted in brain and spinal cord lesions: Ultrastructural, immunohistochemical, and diffusion studies. Tissue Eng 1999;5:467.
33. Osanai T, Kuroda S, Yasuda H, Chiba Y, Maruichi K, Hokari M, Sugiyama T, Shichinohe H, Iwasaki Y. Noninvasive transplantation of bone marrow stromal cells for ischemic stroke: Preliminary study with a thermoreversible gelation polymer hydrogel. Neurosurgery 2010;66:1140.
34. Tabesh H, Amoabediny G, Nik NS, Heydari M, Yosefifard M, Siadat SO, et al. The role of biodegradable engineered scaffolds seeded with Schwann cells for spinal cord regeneration. Neurochem Int 2009;54:73.
35. Walker PA, Aroom KR, Jimenez F, Shah SK, Harting MT, Gill BS, Cox CS, Jr. Advances in progenitor cell therapy using scaffolding constructs for central nervous system injury. Stem Cell Rev 2009;5:283.
36. Martinez-Ramos C, Lainez S, Sancho F, Garcia Esparza MA, Planells-Cases R, Garcia-Verdugo JM, Gomez Ribelles JL, Salmeron Sanchez M, Monleon Pradas M, Barcia JA. Differentiation of postnatal neural stem cells into glia and functional neurons on laminin-coated polymeric substrates. Tissue Eng Part A 2008;14:1365.
37. Soria JM, Martinez-Ramos C, Salmeron Sanchez M, Benavent V, Campillo Fernandez A, Gomez Ribelles JL, Garcia Verdugo JM, Pradas MM, Barcia JA. Survival and differentiation of embryonic neural explants on different biomaterials. J Biomed Mater Res A 2006;79:495.
38. Soria JM, Martinez-Ramos C, Bahamonde O, Garcia Cruz DM, Salmeron Sanchez M, Garcia Esparza MA, Casas C, Guzmán M, Navarro X, Gómez Ribelles JL, García Verdugo JM, Monleón Pradas M, Barcia JA. Influence of the substrate's hydrophilicity on the in vitro Schwann cells viability. J Biomed Mater Res A 2007;83:463.

39. Lluch AV, Fernandez AC, Ferrer GG, Pradas MM. Bioactive scaffolds mimicking natural dentin structure. J Biomed Mater Res B Appl Biomater 2009;90:182.
40. Vidaurre A, Castilla Cortázar I, Meseguer J. Water Sorption properties of poly(ethyl acrylate-*co*-hydroxyethyl methacrylate) macroporous hydrogels. Macromol Symp 2003;283–290.
41. Rodriguez Hernandez JC, Serrano Aroca A, Gomez Ribelles JL, Pradas MM. Three-dimensional nanocomposite scaffolds with ordered cylindrical orthogonal pores. J Biomed Mater Res B Appl Biomater 2008;84:541.
42. Gritti A, Galli R, Vescovi AL. Cultures of stem cells of the central nervous system. Protocols for Neural Cell Culture, 3rd Ed. S. Fedoroff and A. Richardson. Humana Press, Inc., Totowa, NJ. 2001. p 173–197.
43. Paxinos G, Watson C, Pennisi M, Topple A. Bregma, lambda and the interaural midpoint in stereotaxic surgery with rats of different sex, strain and weight. J Neurosci Methods 1985;13:139.
44. Hsu SH, Su CH, Chiu IM. A novel approach to align adult neural stem cells on micropatterned conduits for peripheral nerve regeneration: A feasibility study. Artif Organs 2009;33:26.
45. Yu D, Silva GA. Stem cell sources and therapeutic approaches for central nervous system and neural retinal disorders. Neurosurg Focus 2008;24(3-4):E11, 23 pp.
46. O'Keeffe FE, Scott SA, Tyers P, O'Keeffe GW, Dalley JW, Zufferey R, et al. Induction of A9 dopaminergic neurons from neural stem cells improves motor function in an animal model of Parkinson's disease. Brain 2008;131:630.
47. Lindvall O, Bjorklund A. Cell therapy in Parkinson's disease. NeuroRx 2004;1:382.
48. Lindvall O, Bjorklund A. Cell replacement therapy: Helping the brain to repair itself. NeuroRx 2004;1:379.
49. Hashimoto T, Suzuki Y, Kitada M, Kataoka K, Wu S, Suzuki K, et al. Peripheral nerve regeneration through alginate gel: Analysis of early outgrowth and late increase in diameter of regenerating axons. Exp Brain Res 2002;146:356.
50. Nieuwenhuys R, Voogd J, Van Huijzen C. The Human Central Nervous System, 4th ed. New York: Springer; 2007. p 967.
51. Bai F, Wang Z, Lu J, Liu J, Chen G, Lv R, Wang J, Lin K, Zhang J, Huang X. The correlation between the internal structure and vascularization of controllable porous bioceramic materials in vivo: a quantitative study. Tissue Eng Part A. 2010;16:3791–3803.
52. Malda J, Klein TJ, Upton Z. The roles of hypoxia in the in vitro engineering of tissues. Tissue Eng. 2007;13:2153–2162.
53. Suhonen JO, Peterson DA, Ray J, Gage FH. Differentiation of adult hippocampus-derived progenitors into olfactory neurons in vivo. Nature 1996;383:624–627.